

Catalytic Strategy of Citrate Synthase: Subunit Interactions Revealed as a Consequence of a Single Amino Acid Change in the Oxaloacetate Binding Site[†]

Linda C. Kurz,^{*,‡} Saurabh Shah,[‡] Carl Frieden,[‡] Tanuj Nakra,[‡] Richard E. Stein,[‡] George R. Drysdale,[‡] Claudia T. Evans,[§] and Paul A. Srere[§]

Department of Biochemistry and Molecular Biophysics, Division of Biology and Biomedical Sciences, Washington University School of Medicine, St. Louis, Missouri 63110, and Pre-Clinical Science Unit, Department of Veterans Affairs Medical Center, and Biochemistry Department, University of Texas Southwestern Medical Center, 4500 South Lancaster Road, Dallas, Texas 75216

Received May 4, 1995; Revised Manuscript Received August 7, 1995[®]

ABSTRACT: The active site of pig heart citrate synthase contains a histidine residue (H320) which interacts with the carbonyl oxygen of oxaloacetate and is implicated in substrate activation through carbonyl bond polarization, a major catalytic strategy of the enzyme. We report here the effects on the catalytic mechanism of changing this important residue to glycine. H320G shows modest impairment in substrate Michaelis constants [(7–16)-fold] and a large decrease in catalysis (600-fold). For the native enzyme, the chemical intermediate, citryl-CoA, is both hydrolyzed and converted back to reactants, oxaloacetate and acetyl-CoA. In the mutant, citryl-CoA is only hydrolyzed, indicating a major defect in the condensation reaction. As monitored by the carbonyl carbon's chemical shift, the extent of oxaloacetate carbonyl polarization is decreased in all binary and ternary complexes. As indicated by the lack of rapid H320G–oxaloacetate catalysis of the exchange of the methyl protons of acetyl-CoA or the *pro-S*-methylene proton of propionyl-CoA, the activation of acetyl-CoA is also faulty. Reflecting this defect in acetyl-CoA activation, the carboxyl chemical shift of H320G-bound carboxymethyl-CoA (a transition-state analog of the neutral enol intermediate) fails to decrease on formation of the H320G–oxaloacetate–carboxymethyl-CoA ternary complex. Progress curves and steady-state data with H320G using citryl-CoA as substrate show unusual properties: substrate inhibition and accelerating progress curves. Either one of two models with subunit cooperativity [Monod, J., Wyman, J., & Changeux, J.-P. (1965) *J. Mol. Biol.* 12, 88; Koshland, D. E., Jr., Nemethy, G., & Filmer, D. (1966) *Biochemistry* 5, 365] quantitatively accounts for both the initial velocity data and the individual progress curves. The concentrations of all enzyme forms and complexes are assumed to rapidly reach their equilibrium values compared to the rate of substrate turnover. The native enzyme also behaves according to models for subunit cooperativity with citryl-CoA as substrate. However, the rates of formation/dissociation and reaction of complexes are kinetically significant. Comparisons of the values of kinetic constants between the native and mutants enzymes lead us to conclude that the mutant less readily undergoes a conformation change required for efficient activation of substrates.

Citrate synthase (CS),¹ which catalyzes the condensation of acetyl-CoA (AcCoA) with oxaloacetate (OAA), is the most thoroughly studied of the Claisen enzymes (Scheme 1). The enzymes of this class catalyze the reaction of an electrophilic carbonyl carbon with a nucleophilic carbon derived from a thioester. The direct product of the condensation reaction, citryl-CoA (CitCoA), is hydrolyzed in a second step. The chemical intermediate, CitCoA, is never released from the enzyme. The hydrolysis of the thioester, malyl-CoA, is also catalyzed by the enzyme, but no reversal of the condensation occurs with this unnatural substrate.

Activation of the substrates is a major catalytic strategy of citrate synthase. Structural (Remington *et al.*, 1982) and spectroscopic (Kurz *et al.*, 1985; Kurz & Drysdale, 1987) studies of OAA–CS complexes show that the enzyme achieves significant polarization of the OAA carbonyl bond, thereby increasing the positive charge on the carbonyl carbon and enhancing reactivity toward the condensation with the nucleophilic center of the second substrate, AcCoA. CS also facilitates formation of an effective nucleophilic center in the second substrate, AcCoA. Solid state (Karpusas *et al.*, 1990, 1991) and solution-state studies (Kurz *et al.*, 1992a,b) point to a neutral enol intermediate (or its equivalent) as the activated form of AcCoA.

Evidence has also been accumulating that enzyme conformational changes occurring during the catalytic cycle are essential parts of the catalytic strategy. Some kind of spatial rearrangement of catalytic residues and/or changes in their protonation states seem to be required for efficient enzyme action. A single active site of citrate synthase functions efficiently in apparently conflicting roles, as ligase for AcCoA and OAA and then as hydrolase for CitCoA (Scheme

[†] Supported by National Institutes of Health Grants GM33851 (L.C.K.) and DK13332 (C.F.) and by Grants from Department of Veterans Affairs (P.A.S. and C.T.E.), NIDDK, and NSF (P.A.S.). The Washington University High Resolution NMR Service Facility is funded in part through an NIH Biomedical Research Support Shared Instrument Grant 1 S10 RR02004 and a gift from the Monsanto Company.

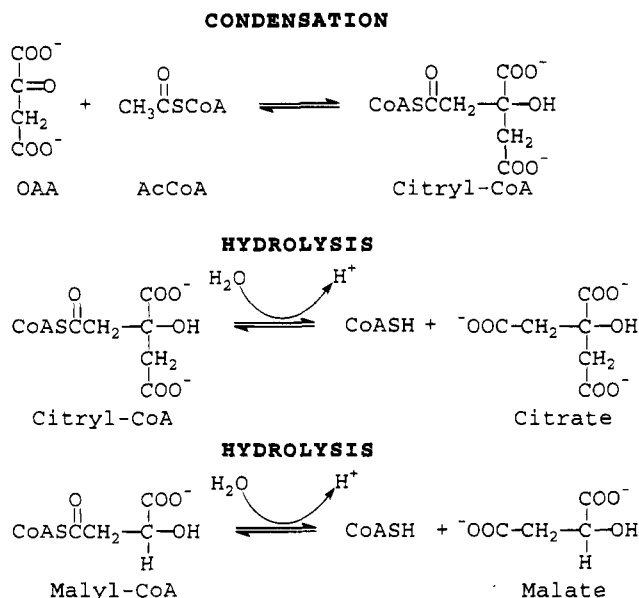
[‡] Washington University School of Medicine.

[§] University of Texas Southwestern Medical Center.

[®] Abstract published in *Advance ACS Abstracts*, October 1, 1995.

¹ Abbreviations: AcCoA, acetyl coenzyme A; CD, circular dichroism; CitCoA, (3S)-citryl coenzyme A; CMCoA, carboxymethyl coenzyme A; CoA, coenzyme A; CS, citrate synthase; DTNB, 5,5'-dithiobis(2-nitrobenzoic acid); OAA, oxaloacetate; cMDH, cytosolic malate dehydrogenase.

Scheme 1. Reactions Catalyzed by Citrate Synthase



1). In the first half of the cycle, the enzyme must activate AcCoA to facilitate the condensation without also catalyzing its hydrolysis. The same acid/bases that interact with AcCoA in the first step facilitate CitCoA hydrolysis in the second step. Many of the *activated* substrates and chemical intermediates implicated in the mechanism of citrate synthase either could not form or would be too unstable in the presence of bulk solvent water. Successive conformation changes must thus occur to exclude or admit water from the active site. Indeed, the X-ray structures of CS fall into one of two conformational classes. The "open" form of the enzyme gives solvent free access to the active site. The "closed" conformation type (there are several slightly different structures in this class) totally excludes bulk solvent with the active site over 15 Å from the nearest surface water contact. The conversion of the open to closed forms is approximated by an 18° rotation of the small domain with respect to the large domain (Remington *et al.*, 1982; Wiegand *et al.*, 1984; Wiegand & Remington, 1986; Karpusas *et al.*, 1990, 1991). Current ideas regarding the conformation changes in citrate synthase may be found in El-Kettani *et al.* (1993) and Gerstein *et al.* (1994). Several kinds of spectroscopic evidence (Srere, 1966; Beeckmans & Kanarek, 1983; Kollmann-Koch & Eggerer, 1989) and chemical modification data (Hammond *et al.*, 1986) suggest that OAA triggers this conformation change which is completed when AcCoA binds blocking any access of bulk water to the active site. The active site of this dimeric enzyme in closed-form structures contains substrate-binding determinants from both subunits and is incomplete in open forms. Specifically, the arginine residue (R421') that interacts with the 4-carboxyl of OAA in ternary complexes originates in the other subunit and is pointed away from the active site in open forms.

We now report the effects on the catalytic mechanism of a single-site change in an active-site residue, H320G. This histidine residue interacts with the OAA carbonyl and has been implicated in its polarization (Wiegand *et al.*, 1984; Kurz *et al.*, 1985; Kurz & Drysdale, 1987). The coordinates of this residue differ by more than 5 Å between the closed and open forms of the enzyme.

For CS, formation of the chemical intermediate (CitCoA) complex almost certainly marks the point at which the enzyme switches from ligase to hydrolase. By studying the way in which the enzyme handles CitCoA as substrate, it may be possible to determine the extent to which the defect produced by any single-site change affects the ligase steps, the hydrolase steps, or the essential conformational transition between the enzyme forms. Unlike the native enzyme, the partitioning of the intermediate CitCoA in the H320G mutant is overwhelmingly in favor of the products, citrate and CoA.

With CitCoA as substrate, H320G exhibits kinetic cooperativity, as a consequence of subunit interactions. Data can be explained using either an MWC model (Monod *et al.*, 1965) or a KNF model (Koshland *et al.*, 1966). For the mutant, the formation of all complexes involved in the allosteric equilibrium is rapid compared to chemical transformation. The behavior of the native enzymes is also consistent with these models for cooperativity. However, the formation/dissociation of complexes is not rapid compared to chemical transformation. Using either model, our results suggest that the subunit interactions underlying the cooperative behavior differ significantly in the mutant in comparison with those in the native enzyme. We have tentatively attributed this difference to the mutant's inability to easily undergo the conformation change from open to closed forms.

Several experimental probes now suggest that, while H320G is deficient in its ability to activate the carbonyl of OAA or to stabilize the reactive acetyl-CoA enol, these defects may in major part result from that same conformational defect.

MATERIALS AND METHODS

Enzymes.² Crystalline CS and cMDH from pig heart were obtained from Sigma Chemical Co., St. Louis, MO. Extensive dialysis against the buffer of the experiment was performed with all enzyme samples (including the cMDH used to assess CitCoA reversal). Mutant enzymes were prepared following the procedures described in Evans *et al.* (1988a,b) and Kurz *et al.* (1992b).

Circular Dichroism. Spectra and titration data were collected, and data were analyzed as previously described (Kurz *et al.*, 1992a).

Carbon-13 NMR. ¹³C spectra were obtained at 150.7 MHz using a Varian Unity 600 spectrometer equipped with a 5-mm multinuclear probe. Proton-decoupled spectra were obtained using Waltz decoupling. The temperature of the sample was 10 °C. The sample buffer was 50 mM Tris·HCl, 1 mM EDTA, pH = 7.50 (uncorrected), and included 25% D₂O (for internal lock) and 0.15 M acetonitrile (as internal chemical shift standard). The cyano resonance of the standard was assigned the value of 118.9 ppm. Other details were as described previously (Kurz *et al.*, 1992a).

Proton Exchange from Ternary Complexes of H320G—OAA with AcCoA and Propionyl-CoA. The rate of exchange of the AcCoA methyl protons or the propionyl-CoA methylene protons with solvent deuterons was measured by an NMR technique similar to that described by Srere (1967). The ratio of AcCoA methyl protons lost (by either exchange

² Enzyme concentrations are given in terms of active sites (not the dimer).

or reaction) to the total in the sample is obtained by the ratio of the integrated areas of the acetyl methyl resonance at 2.35 ppm to the pantothenate methyl resonance at 0.85 ppm (Figure 6). Propionyl-CoA exchange data were analyzed in the same way, except the methylene-proton area (centered at 2.6 ppm) was integrated. For AcCoA samples, correction for the amount of reaction was obtained by assaying the sample for CoA using the standard DTNB assay and for citrate using the citric acid kit supplied by Boehringer Mannheim, Inc. The experiments were run in 50 mM potassium phosphate in D₂O, pD = 7.9, to eliminate the buffer proton resonance of our standard Tris buffer. The sample was 7.2 mM thioester, 7 mM OAA, and 2.5 μ M H320G (AcCoA exchange) or 49.5 μ M H320G (propionyl-CoA exchange). Aliquots were withdrawn from the reaction mixture and quenched by dilution and removal of the enzyme. Each aliquot was diluted 1:7 with deuterated buffer and filtered through an Amicon Centricon 30 ultrafiltration unit and then frozen for later CoA, citrate, and NMR analysis. Four samples with extents of reaction up to 25% were used for calculation of the exchange rate relative to the reaction rate for acetyl-CoA. For propionyl-CoA, fraction exchange as a function of time was used directly in a first-order plot to obtain the pseudo-first-order rate constant for exchange.

Substrates and Inhibitors. [2-¹³C]OAA was prepared as described in Kurz *et al.* (1992a). CMCoA and [1-¹³C]-CMCoA were prepared according to Bayer *et al.* (1981) with modifications as described previously (Kurz *et al.*, 1992a).

The correct (3S) diastereomer of the chemical intermediate, CitCoA, was prepared enzymatically from citrate and AcCoA using citrate lyase from *Enterobacter aerogenes* (Sigma) with modifications of the procedure of Löhlein and Eggerer (1982). Citrate lyase (100 units) was separated from the bulk of the serum albumin stabilizer on an S-300-HR Sephacryl column (1.5 \times 100 cm). Fractions were monitored for citrate lyase activity (Bergmeyer, 1983) and for the presence of serum albumin by SDS electrophoresis. Fractions containing citrate lyase activity with minimal albumin contamination were combined and frozen in liquid N₂. Reaction conditions for the synthesis of CitCoA and its isolation by chromatography on AG50 and DEAE Sepharose were as described by Löhlein & Eggerer (1982), except additional EDTA was added to the reaction mixture to remove the Mg²⁺ present in the combined citrate lyase fractions. The fractions from the DEAE Sepharose column that contained pure CitCoA were pooled. The pooled fractions were made 3 mM in potassium aspartate to provide an acid buffer and lyophilized.³ After dissolution in a minimum amount of 1 mM HCl, the CitCoA sample was desalted on a Sephadex G-10 column (0.7 \times 50 cm) equilibrated in 1 mM HCl. Fractions were monitored for CitCoA by absorbance at 260 nm (ϵ = 15.4 mM⁻¹) and for LiCl by conductivity. Salt-free fractions containing CitCoA were stored frozen in liquid N₂. Stock solutions were prepared in 3 mM HCl as CitCoA is most

stable at low pH. CitCoA was added to experimental solutions at neutral pH only at the time of the experiment. CitCoA concentrations were determined enzymatically with CS in the standard DTNB assay on the day of experiments.

L-4-Malyl-CoA was prepared according to a documented procedure (Lynen, 1962; Arps, 1990), with some changes in the preparation of the intermediate, *N*-octanoylcysteamine. The reduction of *N,N'*-dioctanoylcystamine by sodium amalgam was replaced with reduction by sodium borohydride. The disulfide crystals were dissolved in 90% ethanol at 40 °C, and aqueous sodium borohydride was added slowly in aliquots. Acidification neutralized the mixture, leaving the *N*-octanoylcysteamine. The *N,N'*-dioctanoylcystamine crystals melted at 123–124 °C (apparatus calibrated with melting point standards). The original report give a value of 114–115 °C (Lynen, 1962). Subsequently, another source reported 119–120 °C for the melting point of this material (Ohashi *et al.*, 1985). L-4-Malyl-CoA was purified and stored in the same way as CitCoA.

Kinetic Methods. Citrate synthase activity (Srere, 1969) with the normal substrates, OAA and AcCoA, was monitored through the reaction of the sulfhydryl product, CoA, with DTNB producing TNB which absorbs at 412 nm (ϵ = 14.1 mM⁻¹; Riddles *et al.*, 1979). Absorbance data were collected using a Cary 3 spectrophotometer whose cell compartment was thermostated at 20 \pm 0.1 °C. Initial velocity data obtained under saturating conditions of one substrate with variation in the concentration of the other were fit by nonlinear regression to eq 1. Data with malyl-CoA as

$$\frac{V_i}{[E]} = \frac{k_{cat}[S]}{K_m + [S]} \quad (1)$$

substrate were collected and analyzed in the same fashion.

Progress curves with CitCoA as substrate were collected using a rapid kinetics spectrometer accessory (Model RX 1000, Applied Photophysics). This accessory is a stopped-flow device equipped with a 1 cm path length flow cell which fits in the compartment of an ordinary spectrophotometer. The absorbance data were collected with the fastest data collection rate (0.033 s per point) available on the Cary 3. Data collection was initiated before the reaction solution was mixed, and readings that were collected before the reaction started were deleted from the data set prior to analysis. Rapid and reproducible mixing was accomplished using a pneumatic ram to advance the drive syringes of the apparatus. CitCoA in 3 mM HCl was mixed with enzyme and other reaction components dissolved in 70 mM Tris buffer, 1.4 mM EDTA, pH 7.50, in a ratio of 1:3.5 such the final reaction solution contained 50 mM Tris·HCl, pH 7.50 (no change in pH). All solutions were thermostated at 20 \pm 0.1 °C.

As a chemical intermediate (Scheme 1) in the citrate synthase reaction (Löhlein-Werhahn *et al.*, 1983), CitCoA may partition back to reactants, OAA and AcCoA, as well as partition forward to products, CoA and citrate, before eventual establishment of thermodynamic equilibrium (which greatly favors the products citrate and CoA). The concentrations of thioesters (AcCoA + CitCoA) are monitored directly through their characteristic absorption at 236 nm ($\Delta\epsilon$ = 4.96 mM⁻¹). CoA produced in the forward reaction is monitored at 412 nm ($\Delta\epsilon$ = 14.1 mM⁻¹) through reaction of the CoA sulfhydryl with the thiol reagent, DTNB (Riddles *et al.*,

³ We have experienced problems with lyophilization of HCl solutions of CitCoA. Such samples may have degraded up to 5%–10% and do not exhibit the same progress curves as they did prior to the procedure. As a consequence of the preferential evaporation of water, lyophilization may expose the sample to very high local acid concentrations which may cause hydrolysis, racemization, or other degradative processes. This problem is averted by addition of an amount of potassium aspartate equivalent to the HCl before lyophilization which buffers the solution between pH 2 and 4.

Table 1: Kinetic Constants for Native CS and H320G with Various Substrates^a

substrate	native CS		H320G	
	K_m (μ M)	k_{cat} (min^{-1})	K_m (μ M)	k_{cat} (min^{-1})
OAA	5.9	10 000	43.0 \pm 2.4	16.5 \pm 0.4
AcCoA	5.1		88.6 \pm 5.6	
malyl-CoA	37 \pm 2	401 \pm 6	33 \pm 4	93 \pm 3
citryl-CoA	<i>b</i>	27 (ss) ^c 6000 (burst) ^d	<i>b</i>	25–50 ^e

^a The standard assay (DTNB detection of CoA) was used in assays for the normal substrates and for malyl-CoA. The thioester absorption disappearance assay was used for CitCoA. ^b K_m is not a meaningful concept for CitCoA as substrate of either enzyme since a hyperbolic substrate concentration dependence of the initial velocity is not observed. See Discussion. ^c Steady-state and initial burst velocities for 0.12 μ M CS and 37.5 μ M CitCoA. ^d Calculated from data obtained by Löhlein-Werhahn *et al.* (1983) using an instrument with a shorter dead-time. ^e Range of initial velocity values observed in the concentration range 200–0.5 μ M CitCoA.

1979). OAA produced by reversal of the condensation reaction is detected by coupling its production with the utilization of NADH ($\Delta\epsilon = 6.22 \text{ mM}^{-1}$) in the reaction catalyzed by cMDH. Care was taken to ensure that rates monitored indirectly (CoA and OAA) were studied under conditions in which the rate of the detection reaction does not significantly limit the rate of signal formation. For OAA production, this condition was met by showing that the progress curves are independent of the concentration of cMDH. For CoA, it is necessary to include the DTNB reaction explicitly in the mechanism simulation, as its second-order nature renders it partially rate limiting in early stages of some progress curves when the concentration of CoA is very low.

Mechanism Simulation. The numerical integration of differential rate equations for specific mechanisms and the generation of simulated progress curves for comparison with experimental data were accomplished using the KINSIM and FITSIM programs (Barshop *et al.*, 1983; Zimmerle *et al.*, 1989). Specific mechanisms used are described in the Discussion.

RESULTS

Kinetic Constants for OAA and Acetyl-CoA. Kinetic constants for the reaction of H320G with normal substrates, OAA and AcCoA, were obtained from nonlinear regression fits to eq 1 of initial velocity data obtained over a range of substrate concentrations. The kinetic constants obtained are reported in Table 1. The K_m values for OAA and AcCoA differ substantially from those of the native CS. Therefore, the activity of the mutant preparation cannot be ascribed to contamination with the native CS.

Kinetic Constants for Malyl-CoA. Progress curves obtained with malyl-CoA were normal in all respects for both native CS and H320G. Kinetic constants are reported in Table 1 and compared to those of the native enzyme obtained under the same conditions.

As will be discussed later, the kinetic constants for CitCoA are complex. The CitCoA rates listed in Table 1 are included only for comparison with the normally behaving substrates. The CitCoA steady state rates for H320G and the native enzyme are comparable. The overall progress curve shapes are different, however.

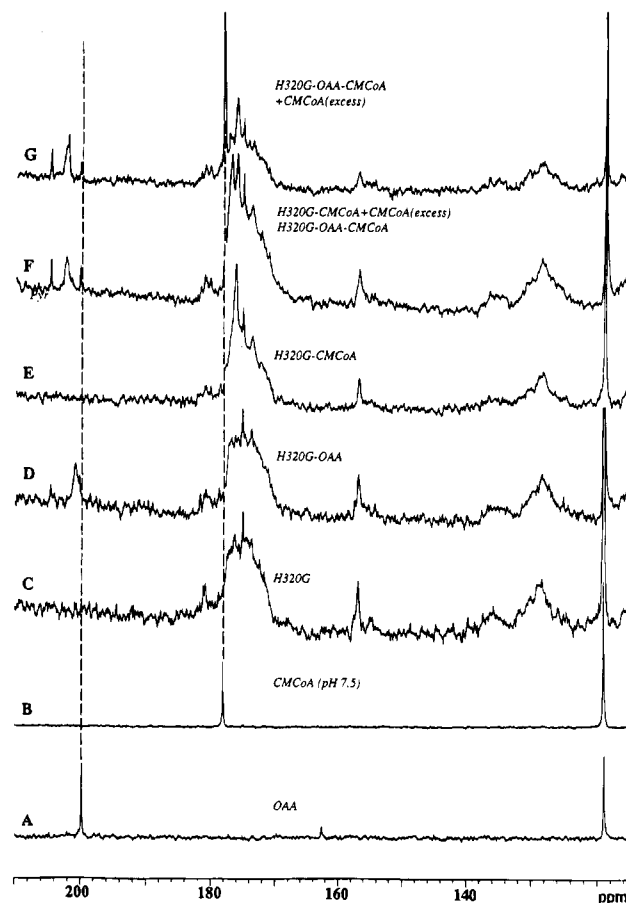


FIGURE 1: ^{13}C spectra of binary and ternary complexes of H320G with OAA and CMCOA. A, 1.78 mM $[2-^{13}\text{C}]\text{OAA}$, 1600 transients; B, 2 mM $[1-^{13}\text{C}]\text{CMCoA}$, 4288 transients; C, 1.8 mM H320G, no ligands, 7040 transients; D, 1.78 mM H320G, 0.9 mM $[2-^{13}\text{C}]\text{OAA}$, 10 240 transients; E, 1.80 mM H320G, 1.6 mM $[1-^{13}\text{C}]\text{CMCoA}$, 8768 transients; F, 1.78 mM H320G, 0.9 mM $[2-^{13}\text{C}]\text{OAA}$, 2.43 mM $[1-^{13}\text{C}]\text{CMCoA}$, 22 720 transients; G, 1.8 mM H320G, 1.6 mM $[2-^{13}\text{C}]\text{OAA}$, 2.43 mM $[1-^{13}\text{C}]\text{CMCoA}$, 8896 transients. Other conditions are described in Materials and Methods. The narrow peak at 204.7 ppm is $[2-^{13}\text{C}]\text{pyruvate}$ from the nonenzymatic decarboxylation of OAA that occurs during the long times required for the collection of protein–ligand data. The narrow peak at 200.3 ppm is a contaminant of the OAA sample which does not bind to the enzyme and rises above the noise only after many transients.

NMR Probes of OAA Polarization by H320G. The OAA carbonyl of the H320G–OAA binary complex (Figure 1D) resonates at 200.7 ppm, which is close to the 199.9 ppm position of the free ligand (Figure 1A). The line width is a full 1 ppm (150 Hz). By contrast, in the native CS–OAA binary complex, the OAA carbonyl resonates at ~ 204 ppm with a line width of 57 Hz (Kurz *et al.*, 1985). Even though OAA binds comparatively loosely to this mutant, the enzyme concentration (1.8 mM) is sufficiently greater than the OAA K_d to eliminate the possibility of an exchange process with the free ligand; there is essentially no free ligand present. The cause of the broad resonance must be sought elsewhere (*vide infra*).

In the ternary complex with the intermediate analog inhibitor, CMCOA, the OAA resonance shifts modestly to 202.3 ppm ($\Delta\delta \approx 1.6$ ppm from the binary position) with little change in line width (Figure 1F,G). In the corresponding ternary complex of the native enzyme, the OAA resonance is found at 206.6 ppm ($\Delta\delta \approx 7$ ppm from the free position) with a line width of 39 Hz (Kurz *et al.*, 1985).

Table 2: Comparison of Specific Rates for Catalysis and Exchange by Citrate Synthase and H320G

	CS		H320G	
	catalysis (min ⁻¹)	exchange (min ⁻¹)	catalysis (min ⁻¹)	exchange (min ⁻¹)
AcCoA		none (AcCoA)		
propionyl-CoA ^c	10 000	7000 (citrate) ^b	17	17
	0.25	300	0.01	0.4

^a Specific rate of exchange was determined by plotting the fraction of AcCoA exchanged *vs* the fraction of reaction. The plot is linear with a slope of 1.03 ± 0.18 (data not shown). Extents of reaction or exchange were kept below about 20% to minimize corrections for multiple exchange. Extents of reaction obtained by determination of CoA or citrate are in good agreement. The first-order rate constant for propionyl-CoA exchange catalyzed by H320G–OAA was calculated from a fit to a first-order exponential rate equation (data not shown). No corrections were required for reaction in this case. ^b No solvent exchange of the methyl protons of AcCoA is observed during conditions of net citrate synthesis in which the overall reaction has been made irreversible by oxidation of CoA (Eggerer, 1965). The methylene of product citrate originating in AcCoA, however, shows 70% exchange (Meyers & Boyer, 1984) also under irreversible conditions *via* reaction of CoA with DTNB. ^c Both native CS and H320G preferentially catalyze the exchange of the *pro-S* methylene proton of propionyl-CoA.

NMR Probes of AcCoA Activation by H320G. In the binary complex (Figure 1 E), the carboxyl of CMCoA is found at 176.1 ppm ($\Delta\delta \approx -2$ ppm from the free position), which is lower than the 177.7 ppm ($\Delta\delta \approx -0.4$ ppm from the free position) observed previously in binary complexes of the native enzyme or of mutants containing changes in the AcCoA-binding residue D375 or H274 (Kurz *et al.*, 1992a,b). The CMCoA binary complexes for all enzymes, including H320G, are in *fast* exchange with free ligand on the NMR time scale (Figure 1F). When excess CMCoA is present in the solution, the binary complex peak moves toward the free position as a consequence of fast exchange averaging with unbound ligand. The sample in Figure 1F is a mixture of (enzyme–CMCoA) binary and (enzyme–OAA–CMCoA) ternary complexes in the presence of excess CMCoA.

In the ternary complex with OAA, the carboxyl resonance of CMCoA is unchanged in position (Figure 1 F,G) in contrast to native CS or D375 mutants where $\Delta\delta \approx -2.9$ to -6.5 ppm from the free position. However, like the native enzyme or AcCoA-site mutants, the CMCoA in this complex with H320G–OAA is in *slow* exchange with free CMCoA on the NMR time scale (Figure 1G).

Proton Exchange Probes of AcCoA Activation by H320G. The specific rate of methyl proton exchange in the ternary H320G–OAA–AcCoA is very low and fortuitously about equal to the low rate at which that complex produces products. The specific rate of exchange for the methylene proton of propionyl-CoA is also small compared to the native CS. These results for both the native enzyme and H320G are summarized in Table 2.

The mutant apparently preserves the stereoselective exchange of the *pro-S* methylene proton previously observed with the native enzyme (Weidman & Drysdale, 1979). That only one of the methylene protons of propionyl-CoA is preferentially exchanged by H320G is shown by the collapse of the triplet from the propionyl-CoA methyl resonance to a doublet with no change in integrated intensity.

CD Spectra and K_d of CMCoA from H320G–OAA. Unlike the native enzyme and mutants in the AcCoA site

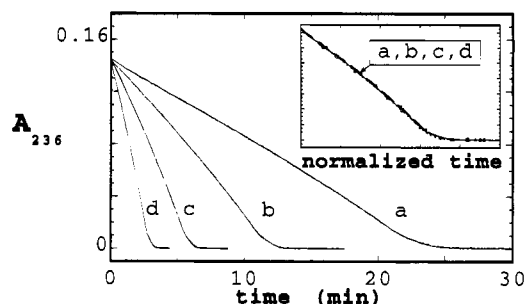


FIGURE 2: Progress curves as functions of enzyme concentration for hydrolysis of 31 μ M CitCoA catalyzed by H320G monitored by disappearance of the thioester absorbance at 236 nm: curve a, 0.042 μ M; curve b, 0.084 μ M; curve c, 0.168 μ M; curve d, 0.336 μ M. Inset, time-normalized progress curves: small dash line and solid squares, 0.042 μ M; medium dash line and open squares, 0.084 μ M; long dash line and solid circles, 0.168 μ M; solid line and solid circles, 0.336 μ M.

which show a small *increase* in CD strength at 260 nm when OAA is added to the free enzyme (Kurz *et al.*, 1992a,b), H320G shows no change or even a small *decrease* (data not shown).

The spectra of the ternary H320G–OAA–CMCoA complex (data not shown) resemble spectra of the native enzyme (Kurz *et al.*, 1992a). CD titration data yield a K_d for CMCoA from the H320G–OAA complex of 0.22 ± 0.04 μ M. This is only 10-fold looser than native enzyme, which has a K_d of 0.023 μ M for dissociation of CMCoA from the CS–OAA complex (Kurz *et al.*, 1992a).

K_d of OAA from H320G–OAA and H320G–OAA–CMCoA. The effect of OAA complex formation on the urea-induced exposure of a reactive sulfhydryl is a convenient method for OAA K_d determinations (Srere, 1966) in a variety of CS binary and ternary complexes. For H320G this method yields a value of 41.2 ± 0.1 μ M for the OAA binary complex in comparison to a value of 1.06 ± 0.07 μ M for the native enzyme (Zhi *et al.*, 1991) using the same method. The dissociation constant of OAA from the H320G–OAA–CMCoA ternary complex is considerably smaller, 6.7 ± 0.2 μ M. OAA dissociation from the native enzyme–OAA–CMCoA complex cannot be detected by this method. The K_m of OAA for H320G determined in the usual kinetic assay is approximately equal to the K_d determined by the urea protection method.

H320G-Catalyzed Hydrolysis of CitCoA. Progress curves for reactant disappearance (thioester absorbance monitored) for a single concentration of CitCoA (31 μ M) at enzyme concentrations² from 0.042 to 0.36 μ M are shown in Figure 2. The rates constantly accelerate until close to substrate depletion. Progress curves for product appearance under the same conditions have been collected using the DTNB reaction to detect CoA. After correction for the fact that the DTNB reaction becomes partly rate limiting for the fastest reactions at the earliest times, product appearance curves (expressed in terms of extent of reaction) are superimposable on the curves for reactant disappearance (data not shown).

The initial velocities are directly proportional to the enzyme concentration. More significantly, the anomalous progress curve *shape* is independent of the enzyme concentration, as is shown by normalizing the time axis of all the runs according to the enzyme concentration (inset of Figure 2). Thus, the accelerated disappearance of substrate does not arise from transient, non-steady-state processes occurring

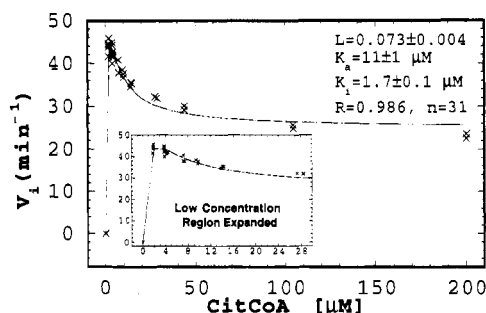


FIGURE 3: Specific initial velocities for hydrolysis of CitCoA as functions of the concentration of CitCoA. The H320G concentration is $0.084 \mu\text{M}$ active sites; solid line, least-squares fit of eq 2 to the data. Inset, the low concentration region expanded; solid line calculated from the least-squares fit of the data to the MWC model (Scheme 2, left).

on the same time scale as the experiments. For example, if a slow isomerization from inactive to active enzyme were taking place, then an increase in initial enzyme concentration would result in completion of the reaction before as much enzyme has been converted to the active form as would have occurred at lower concentration. Less rate acceleration should take place before the substrate was consumed. Since this does not occur, we then conclude that all enzyme complexes must equilibrate rapidly (or reach steady-state concentrations), and the unusual shape of the progress curves must have some other origin.

Although the shape of progress curves is independent of enzyme concentration, the shape *does* depend on CitCoA concentration. Below about $10 \mu\text{M}$, the curves are nearly linear, failing to accelerate noticeably (data not shown).

Specific initial velocities as functions of CitCoA concentration are shown in Figure 3. At high CitCoA concentrations, the rates approach a low constant value. At lower concentrations, the initial rate increases with decreasing concentration. For all concentrations, the value of the specific initial velocity *equals or exceeds* the value of k_{cat} , 17 min^{-1} , of the reaction with the normal substrates, AcCoA and OAA. This is in marked contrast to the behavior of the native enzyme with which the steady-state rate of CitCoA utilization is 50-fold lower than the reaction with the physiological substrates (Pettersson *et al.*, 1989).

At the two lowest CitCoA concentrations reported, 0.5 – $1.0 \mu\text{M}$, the rate values are clearly leveling off. A great deal of effort was expended in unsuccessful attempts to obtain data at even lower CitCoA concentrations. Technical difficulties have prevented data collection in this region where the velocities must decrease.

In contrast to the native enzyme, with which CitCoA is both hydrolyzed and converted back to reactants, H320G does not cleave CitCoA back to reactants. The native enzyme partitions CitCoA initially, with about one in four CitCoA molecules returning to OAA and AcCoA. However, for H320G, the progress curve for CoA appearance is unaffected by the presence of cMDH and NADH and no NADH disappearance is detected, both observations indicating no partitioning of the citryl-CoA to OAA and AcCoA (data not shown).

Initial addition of 0.1 – 0.5 mM citrate to reaction mixtures, exceeding the concentration of CitCoA by 2–10-fold, was without effect on the progress curves. Thus, there is no evidence for citrate activation (or inhibition). The identity

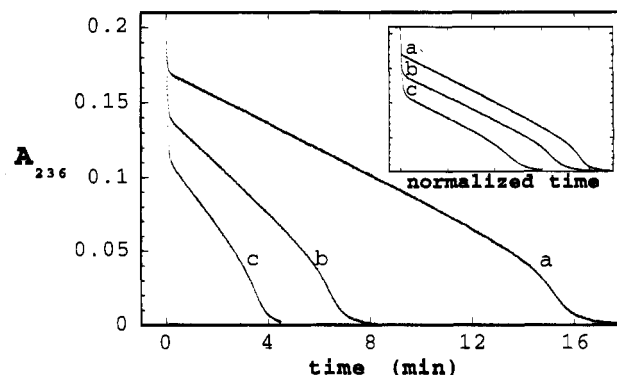


FIGURE 4: Progress curves as functions of enzyme concentration for disappearance of $35 \mu\text{M}$ CitCoA catalyzed by native CS monitored by the thioester absorbance at 236 nm ; curve a, $0.06 \mu\text{M}$; curve b, $0.12 \mu\text{M}$; curve c, $0.16 \mu\text{M}$. Inset, time-normalized progress curves.

of progress curves for CitCoA disappearance and CoA appearance in which CoA was detected by its reaction with DTNB also eliminates CoA activation as a possible explanation for the accelerating time course.

CitCoA as a Substrate of the Native CS. The reaction of CitCoA with native CS has been previously studied (Pettersson *et al.*, 1989; Lill *et al.*, 1987a,b; Löhlein-Werhahn *et al.*, 1983, 1985), and extensive data have been reported by those workers. Progress curves for CitCoA disappearance for various concentrations of native CS are shown in Figure 4. These progress curves have three phases. A rapid burst phase is followed by a nearly linear rate. Near the end of the reaction, a noticeable acceleration occurs. Unlike the corresponding progress curves obtained with H320G, the shape of the native enzyme progress curve *does* depend upon the enzyme concentration (Figure 4, inset). The fraction of the reaction occurring in the burst increases with increasing enzyme concentration. The absolute value of the rate in the linear, steady-state phase is very much slower than would be observed starting with the usual substrates, OAA and AcCoA. In the $0.12 \mu\text{M}$ (curve b) run shown in Figure 4, the specific velocity in the steady-state phase is about 27 min^{-1} in comparison to the $10\,000 \text{ min}^{-1}$ rate with the true substrates. Using different rapid mixing and data collection techniques, Löhlein-Werhahn *et al.* (1983) report a burst velocity value that is 60% of the k_{cat} of the usual substrates, AcCoA and OAA.

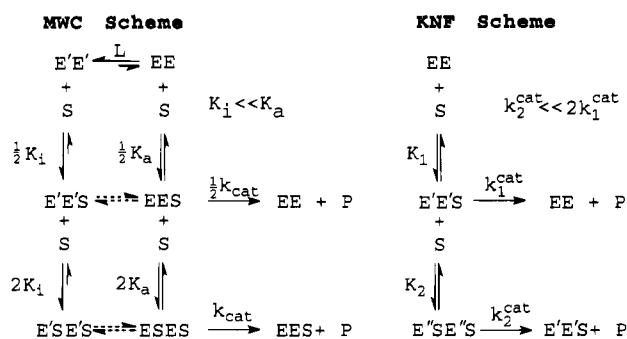
DISCUSSION

H320G Subunit Cooperativity with CitCoA as Substrate. The rate law for the utilization of CitCoA as a substrate by H320G is given by eq 2:

$$\frac{V_i}{[E]} = \frac{c[S]^2 + d[S]}{1 + a[S]^2 + b[S]} \quad (2)$$

Such a rate law containing squared terms in the substrate concentration is characteristic of cooperativity (Neet, 1980). (We do not mean that the enzyme under physiological conditions exhibits sigmoidal kinetics characteristic of regulatory behavior in metabolic pathways.) It may result

Scheme 2. Allosteric Models for the Hydrolysis of CitCoA Catalyzed by H320G



from cooperativity⁴ in the binding of substrate molecules to the dimer, from differences in the turnover constants of singly and doubly ligated enzymes, or from isomerization between two or more forms of the enzyme occurring on a time scale comparable to turnover. While a very general model may eventually prove necessary as more mutants are studied, we explicitly consider here two simplified models (Scheme 2), which satisfactorily explain the data but present rather different physical pictures at the molecular level.

The MWC model (Scheme 2, left) presumes a pre-existing equilibrium between two states of the enzyme described by equilibrium constant, L , each state with a different intrinsic affinity for the substrate. One feature of this model is the lack of a kinetically accessible path between the two forms of ligated macromolecule (indicated by the dashed equilibria in Scheme 2, left). Another feature is the absence of mixed conformers: after substrate binds to one subunit of either the active or the inactive conformational form, the other subunit of the dimer is locked into that form.

Subunit cooperativity according to this MWC model predicts all the features of the steady-state and progress curve data.⁵ The initial velocity equation has the form of eq 2. To produce substrate inhibition, the enzyme form with higher substrate affinity is catalytically inactive. Substrate inhibition in initial velocity data and release of that inhibition causes accelerating progress curves as the substrate concentration drops in full time course experiments. The initial velocity levels off to a constant value at high substrate concentrations (data shown in Figure 3). At very low substrate concentrations, the model predicts a normal second-order rate law (and consequently a normal non-accelerating progress curve), as

⁴ Explanations not involving subunit interactions are unlikely. A classic explanation for substrate inhibition invokes two substrate molecules binding to a single active site. The tight binding of CitCoA (both to the native enzyme and H320G) together with the structures of all the known CS complexes and the lack of total inhibition at high CitCoA concentration renders this explanation very unlikely. All of the complexes containing ligands with binding determinants from both substrates are "closed" (including the one with an unreactive CitCoA analog), and there is simply no room to accommodate two CitCoA molecules within a single active site (Remington *et al.*, 1982). Another mechanism with substrate inhibition resulting from conformation changes at a single active site, the mnemonic enzyme concept (Ricard *et al.*, 1974), does predict the observed form of the substrate concentration dependence for initial velocity experiments. This mechanism relies on a conformation form induced by product formation at a single site that persists for a time after the product is released. If such a state of affairs were operative in the case of H320G, the inclusion of product in the reaction mixtures would effect the shape of progress curves contrary to observation. The mnemonic mechanism has also been ruled out in the case of the native CS with a similar argument (Löhlein-Werhahn *et al.*, 1983).

would be observed with Michaelis–Menten kinetics (data not shown).

The allosteric equilibrium favors the inactive form of H320G. Nonlinear regression fits of the steady-state data (Figure 3) yields values of 0.073 ± 0.004 for L and values of 10.5 ± 1.0 and $1.7 \pm 0.1 \mu\text{M}$ for K_a and K_i , respectively. The individual progress curves are also well described by the same mechanism. A progress curve for hydrolysis of $26 \mu\text{M}$ CitCoA by $0.08 \mu\text{M}$ H320G is shown in Figure 5, panel A. The dotted line is the nonlinear regression fit of the data obtained using the kinetic simulation and fitting programs KINSIM and FITSIM.

The KNF model (Scheme 2, right) also involves conformation changes. However, these are sequentially induced by ligand binding (Koshland *et al.*, 1966) i.e., the various conformers do not pre-exist at significant concentrations. Substrate inhibition and the limiting behavior at low and high substrate concentrations are predicted if the conformation state of the dimeric enzyme with two substrate molecules is

⁵ The initial velocity equation in terms of the parameters of the MWC model is given by eq 3.

$$\frac{V_i}{[E]} = \frac{\left(\frac{Lk_{cat}}{(L+1)K_a^2}\right)[S]^2 + \left(\frac{Lk_{cat}}{(L+1)K_a}\right)[S]}{1 + \left(\frac{2LK_i + 2K_a}{(L+1)(K_iK_a)}\right)[S] + \left(\frac{LK_i^2 + K_a^2}{(L+1)(K_i^2K_a)}\right)[S]^2} \quad (3)$$

This expression predicts that the initial velocity levels off to a constant value at high substrate concentrations as shown in eq 4 (data shown in Figure 3).

$$\text{As } [S] \rightarrow \infty, \quad \frac{V_i}{[E]} \rightarrow \frac{LK_i^2k_{cat}}{LK_i^2 + K_a^2} \quad (4)$$

At very low substrate concentrations, the model predicts, eq 5, a normal second order rate law (and consequently a normal nonaccelerating progress curve) as would be observed with Michaelis–Menten kinetics (data not shown).

$$\text{As } [S] \rightarrow 0, \quad \frac{V_i}{[E]} \rightarrow \left(\frac{k_{cat}[S]}{K_a}\right)\left(\frac{L}{L+1}\right) \quad (5)$$

The apparent second-order rate constant however, differs from the usual k_{cat}/K_a by the term, $L/(L+1)$.

A quantitative fit of the data to this model requires an assumption concerning the value of k_{cat} . For this purpose, we use the relative abilities of native and mutant enzymes to catalyze the hydrolysis of maly-CoA. Maly-CoA (Scheme 1) is a simple hydrolysis substrate (no reversal of condensation) for both native and mutant enzymes. Furthermore, it has normal progress curves and a Michaelis–Menten substrate concentration dependence. The K_m values are equal for both enzymes, while the k_{cat} values differ by about 4-fold. Pettersson *et al.* (1989) assign a rate constant of $50\,000 \text{ min}^{-1}$ to the forward rate constant for CitCoA hydrolysis by native CS, a value consistent with all known kinetic data but not rigorously determined by them. We set the value of k_{cat} for CitCoA as a hydrolysis substrate for H320G 4-fold lower than this, at $12\,500 \text{ min}^{-1}$. The values of K_a and K_i are relatively insensitive to the choice of value for k_{cat} . The value of L is sensitive; a k_{cat} of $50\,000$ lowers the L value to 0.018.

The initial velocity expression for the KNF model is given by eq 6.

$$\frac{V_i}{[E]} = \frac{\frac{k_2^{cat}}{K_1K_2}[S]^2 + \frac{k_1^{cat}}{K_1}[S]}{1 + \frac{1}{K_1}[S] + \frac{1}{K_1K_2}[S]^2} \quad (6)$$

The limiting velocities of the KNF mechanism are given by k_2^{cat} at high substrate concentrations and by k_1^{cat}/K_1 at low substrate concentrations.

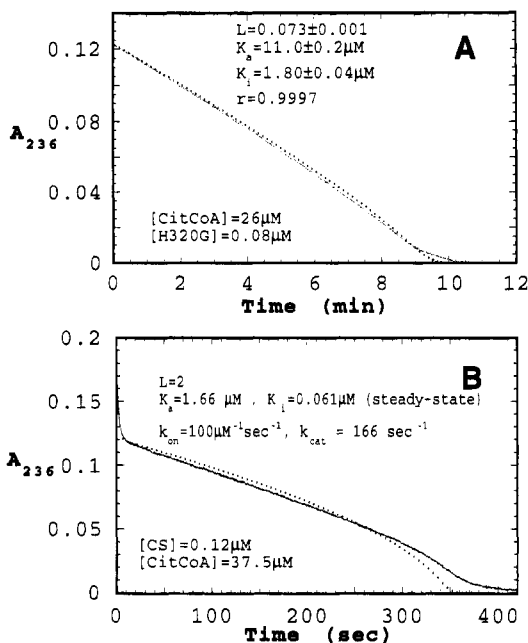
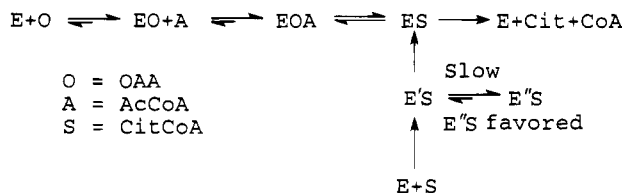


FIGURE 5: A, progress curve for 26 μM CitCoA as substrate for 0.08 μM H320G. Dotted line is the curve generated by the nonlinear regression and simulation programs KINSIM and FITSIM using the MWC mechanism (Scheme 2, left). The simulated curve was calculated from the parameters given in the figure. B, progress curve for 37.5 μM CitCoA as substrate for 0.12 μM CS. Dotted line is the curve generated by the program KINSIM for the steady-state MWC model. The simulated curve was calculated from the parameters given in the figure.

Scheme 3. Noncooperative Model for Hydrolysis of CitCoA Catalyzed by Native CS



bound such that its turnover rate (k_{cat}) is less than twice that for the form with only one substrate ligand. All the features of the data are equally predicted by the KNF model.⁵ Nonlinear regression fit of the data yields values of 46.3 ± 2.1 and 21.3 ± 1.1 for k_1^{cat} and k_2^{cat} , respectively, and values of 0.0 ± 0.08 and 19.1 ± 5.1 for K_1 and K_2 , respectively.

Native CS Subunit Cooperativity with CitCoA as Substrate. CitCoA as a substrate of native CS has been extensively studied by Eggerer's group (Pettersson *et al.*, 1989, and references therein). These workers developed a mechanism without cooperativity (Scheme 3) which semiquantitatively accounts for all of the features of the native CS progress curves. Their mechanism requires formation of three different enzyme complexes of CitCoA, two of which are inactive, together with a slow, reversible isomerization between two of the inactive forms.

Our efforts to apply the Pettersson mechanism to the H320G data have been unsuccessful. The steady-state initial velocity equation for the Pettersson mechanism does not contain squared terms in the substrate concentration.

The native CS progress curves are also consistent with allosteric mechanisms, although we have to make a number of assumptions and omit some known complexities.⁶ The dotted line of Figure 5, panel B, is a simulation of CitCoA

disappearance using a steady-state version of the MWC mechanism. In contrast to the results for H320G (panel A), the allosteric equilibrium for the native CS favors the active enzyme.

The KNF scheme also reproduces the form of the native CS progress curves. The slow buildup of the relatively inactive doubly ligated enzyme accounts for the burst in the native enzyme progress curves and its predominance during the steady-state accounts for the observed inhibition. The inhibition is relieved as the substrate concentration drops at the end of the reaction and the concentration of active single-ligand enzyme builds up. The KNF model preserves many of the features of the original Pettersson mechanism with the addition of subunit interactions.

It is very difficult to distinguish between these two models which describe cooperative behavior. While both emphasize the importance of conformational equilibria, the models differ in whether the conformational equilibria pre-exist or occur only as a consequence of ligand binding. Transient-state experiments and data with other mutants could very well mandate a hybrid model, perhaps with features from both. For other mutants, slow isomerization (Neet, 1980) between enzyme forms may also have to be considered.⁷

Molecular Basis for Subunit Interactions in Citrate Synthase. What are the structures of these conformations which we have identified in both the native and mutant enzymes? We have presumed that they are the closed and open forms that have been characterized by crystallography. However, X-ray structures of H320G and its complexes are not available. Theoretical calculations may be able to give additional insight into the structures of these conformers.

A feature of the MWC model is the control of the fate of an empty subunit once the ligand is bound to the other. If one subunit is in a given conformation, then the other would be locked into a like state. For citrate synthase, this property is entirely reasonable on structural grounds, as the active site contains residues from both subunits (Wiegand *et al.*, 1984) of this dimeric enzyme. This same argument may also be invoked to rationalize the KNF model in which the

⁶ A number of simplifications and assumptions were made. The most serious simplification is that Scheme 2 ignores the partitioning of the substrate in two directions. Since 75%–80% of the initial product is CoA, this simplification has less importance for the earlier parts of the progress curve but will become more serious later on as the concentrations of AcCoA and OAA build up relative to CitCoA. The two-substrate nature of the natural reaction is ignored along with the possibility of mixed substrate–product complexes. For this simulation, we have set the association rate constants k_{on}^{A} and k_{on}^{S} at a value of $100 \text{ s}^{-1} \mu\text{M}^{-1}$ (approximating encounter-control). Statistical factors are set exactly. The value of k_{cat} of 166 s^{-1} was taken as the value for the natural reaction when both subunits are saturated with substrate. The kinetic constants shown in Figure 5, panel B, produce substrate inhibition in the steady-state phase only at very low substrate concentrations, below those easily studied.

It is possible that appropriate inclusion of the omitted complexities in the mechanism would result in more satisfactory fits. However, the number of parameters for a more complex model is large compared to the number of experiments. Over 36 rate constants result even if the binding of OAA and AcCoA is not considered separately. Even though inclusion of statistical factors reduces the number of independent parameters by about half, there is no real justification for this assumption. Furthermore, it is technically difficult to include this complexity at the present time. For these more complex models, the Gear algorithm fails (hanging up the calculation) for many combinations of parameters.

⁷ Recent transient-state experiments at high enzyme concentrations indicate that burst kinetics may be present in some H320 mutants.

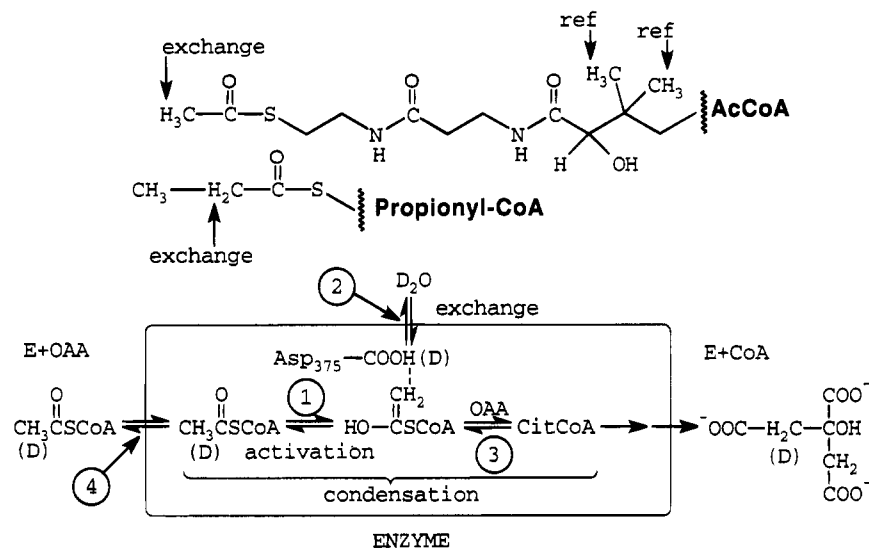


FIGURE 6: Citrate synthase reaction emphasizing the processes affecting the detection of solvent exchange of the AcCoA methyl protons.

enzyme undergoes conformation changes at each ligand-binding step. If tight-binding CitCoA induces the closed conformation, the second CitCoA binds slowly, but, once bound, the closed form of both subunits is greatly stabilized. Turnover from this double-ligand enzyme is greatly slowed because products may only be released from the open form, a transition made very difficult if the other subunit contains unreacted CitCoA.

Clues of the reality of such a physical picture have been noted previously (Löhlein-Werhahn *et al.*, 1988). Tight binding of the chemical intermediate and/or substrates seems to be required for observation of the anomalous kinetic pattern (burst, low steady-state rate, final acceleration). Limited proteolysis of the enzyme (Löhlein-Werhahn *et al.*, 1983; Lill *et al.*, 1984) "normalizes" the kinetic data for CitCoA while simultaneously greatly increasing the K_m for AcCoA (from 6 to 60 μ M or 1 mM, depending on the site of proteolysis). This result is reasonable if the closed form of the proteolyzed enzyme is less stable. The kinetic data for malyl-CoA are normal Michaelis-Menten (Löhlein-Werhahn *et al.*, 1983). Malyl-CoA lacks the methylene and carboxylate which originate from the 3- and 4-carbons of OAA (Scheme 1). It is the 4-carboxylate of OAA that interacts with R421' (Wiegand *et al.*, 1984) of the other subunit, an interaction present only in closed forms. Furthermore, malyl-CoA binds relatively loosely ($K_m = 40 \mu$ M; Löhlein-Werhahn *et al.*, 1983; this work) in comparison with CitCoA. Malyl-CoA hydrolysis may occur from an open enzyme or from a less stable closed form. Citrate synthases from several bacterial sources (such as the *Escherichia coli* enzyme) do not show the anomalous kinetic pattern (Löhlein-Werhahn *et al.*, 1988). These enzymes have relatively high K_m values for CitCoA hydrolysis (and for the normal substrates as well). Again, their closed forms may be less stable. In contrast, the yeast enzyme has high affinity for its substrates and shows anomalous kinetics for CitCoA hydrolysis similar to those observed with the mammalian enzymes (Löhlein-Werhahn *et al.*, 1988).

Catalytic Defect in H320G Is in the Condensation Step. The observed (inhibited) rates of CitCoA hydrolysis are $\geq k_{cat}$ starting from the normal substrates. While there is some impairment in the hydrolase activity, it is comparatively modest. The value of k_{cat} for malyl-CoA hydrolysis catalyzed

by the mutant is about 25% of that for native CS, while the mutant's ability to catalyze the overall reaction is considerably smaller; k_{cat} for H320G < 0.001 of that for native CS. The partitioning of the chemical intermediate, CitCoA, back to OAA is very difficult because the rate constant for the reverse condensation is very small. A lower rate constant for the reverse condensation in comparison to the situation in the native enzyme (partitioning back to reactant OAA is readily observed in native CS) is almost certainly a consequence of a higher free energy of the condensation transition state than in native CS.

Activation of Both Substrates Impaired. With the major defect in the overall condensation reaction, the enzyme fails to properly activate one or the other or both substrates. Certainly the mutant fails to properly activate OAA by carbonyl polarization, even in complexes with the transition-state inhibitor, CMC₂CoA. The ¹³C chemical shift of the carbonyl of OAA remains close to the free solution value in both binary and ternary complexes. This is in contrast to the behavior of native CS in which the ~7 ppm deshielding of the OAA carbonyl reflects reduction in its π -bond order, from 2 to 1.7, in the ternary complex with CMC₂CoA.

The slow rate of AcCoA methyl proton and propionyl-CoA methylene proton solvent exchange catalyzed by H430G (Table 2) indicates a serious defect in the ability of H320G to generate the AcCoA intermediate. Exchange experiments unambiguously monitor thioester activation only under certain circumstances, which, we argue, are met in the case of H320G. Four processes (Figure 6) can contribute to the observed rate of exchange: (1) The rate of removal of the methyl proton of AcCoA and its reprotonation by the active site base, D375; (2) The rate of exchange of the D375 proton with bulk solvent, presumably via a conformation change; (3) The association and dissociation of AcCoA from the enzyme (the exchanged ligand must dissociate from the enzyme to be detected); (4) The forward and reverse rates of the condensation step producing CitCoA. Only the first of these processes monitors the enzyme's ability to activate AcCoA.

Data obtained with the native CS, indicate that the rate of exchange of the D375 proton (process 2) must be relatively fast and is thus unlikely to be rate determining in the mutant. For the native CS-OAA-AcCoA complex, no solvent

exchange of the AcCoA methyl protons are observed (Eggerer, 1965), but 0.7 solvent proton appear in the methylene of citrate (Meyers & Boyer, 1985). The experiments were run under irreversible conditions, removing the CoA as it was released (either by oxidation or by reaction with DTNB). No AcCoA exchange is observed because bound (exchanged) AcCoA is never released before product formation. The exchange observed in citrate must then occur from some ternary complex of the enzyme. In that ternary complex, the protonated active-site base must have relatively free access to solvent protons.

Unlike native CS, the H320G exchange data cannot contain a contribution from the step producing CitCoA (process 4) since we have demonstrated that CitCoA reversal does not occur to a measurable extent and that lack of OAA polarization must greatly reduce the forward condensation rate constant as well (*vide supra*). Dissociation of AcCoA from the enzyme is not rate limiting (process 3). Note the relative high K_m values (and low overall k_{cat} and the absence of any major defect in the hydrolysis step). Thus, the activation of AcCoA is the most important step contributing to the observed (slow) rate of solvent exchange.

If OAA activation were completely independent of thioester activation, then we would have expected very rapid exchange. The slow step would be the actual condensation of the properly activated thioester with the improperly activated OAA. The free reversal of the steps prior to the kinetic block should have resulted in fast exchange. However, since slow exchange is observed we conclude that AcCoA activation is impaired in the mutant. The propionyl-CoA exchange data lead to the same conclusion.

NMR data with CMCoA complexes are also consistent with a defect in the ability of the mutant to stabilize the activated form of AcCoA. In the native CS and previously studied mutants, the chemical shift of the *binary* CMCoA complex is close to the free solution value (anion). In *ternary* complexes of native CS and D375 mutants, the CMCoA carboxyls have lower chemical shifts, close in value to that of the protonated acid. Together with structural (Karpusas *et al.*, 1990) and other solution evidence, these data led to the proposal that acetyl-CoA enol (or possibly a strong hydrogen-bonded enolate) is the activated intermediate (Kurz *et al.*, 1992a,b). The decrease of the value of the chemical shift of the CMCoA carboxyl is the feature that distinguishes it as a transition-state analog inhibitor in *ternary* complexes. Thus we were surprised to find the same chemical shift value (176.1 ppm) for *both* binary and ternary complexes of an OAA site mutant, H320G.

The value of the CMCoA chemical shift of H320G–OAA–CMCoA may have the same value in *both* binary and ternary complexes because the protein conformation change, which normally is initiated by the binding of OAA and leads to the activation of AcCoA, either does not occur at all or occurs incorrectly. The binary complex is in fast exchange, while the ternary complex is in slow exchange on the NMR time scale, even though the chemical shift values are identical in both complexes. Our NMR chemical shift exchange data (Figure 1) thus suggest that the conformation change occurs incorrectly so as not to properly activate AcCoA but does slow the dissociation rate of CMCoA from the ternary complex.

Conformation Defect Suggested by CD Data. Although the change in the native protein CD spectrum induced by

OAA binding is small, its failure to occur in H320G may be an accurate indication of a global conformational defect in that mutant. The fact that the CD spectra of the ternary OAA–CMCoA complexes are the same while the binary OAA complexes differ does not imply, however, that the proper conformation is adopted in the active-site region, even in that ternary complex. The CD spectra of the OAA binary and OAA–CMCoA ternary complexes are sensitive to different aspects of the structures of those complexes. The ternary complex spectrum is dominated by the protein-induced CD of the adenine chromophore. It seems probable that the adenine binding environment, responsible for the induced CD, is more or less independent of interactions in the active site. The changes in the CD spectrum which occur when the OAA binary complex is formed originate *from the protein itself* since the ligand has no chromophore in this region.

Conclusion. Subunit interactions within the dimeric citrate synthase are revealed when H320, a residue that is important in OAA binding, is replaced with glycine. While we believe these subunit interactions also occur in the native enzyme, only the mutant data *require* a cooperativity mechanism for their explanation. The cooperative CitCoA kinetics suggest that the predominant conformation state of this mutant enzyme is inactive (MWC model) or that the mutant is unable to properly close (KNF model). The catalytic defect in H320G lies primarily in the condensation step; the rate of the hydrolysis step is only mildly effected. Within the condensation step itself, the activations of both substrates are impaired. With H320G, thioester activation is not independent of OAA activation. A defect in the OAA binding site is propagated into the binding site for AcCoA. We propose that an enzyme conformation change, which is triggered by OAA binding and leads to AcCoA activation, fails to occur efficiently with this mutant. Conformation changes and activation of both substrates are linked.

ACKNOWLEDGMENT

We gratefully acknowledge the critical comments of Professors Hermann Eggerer and Gösta Pettersson on an earlier version of this manuscript.

REFERENCES

- Arps, P. J. (1990) *Methods Enzymol.* 188, 386–391.
- Barshop, B. A., Wrenn, R. F., & Frieden, C. (1983) *Anal. Biochem.* 130, 134.
- Bayer, E., Bauer, B., & Eggerer, H. (1981) *Eur. J. Biochem.* 120, 155.
- Beeckmans, S., & Kanarek, L. (1983) *Int. J. Biochem.* 15, 1119.
- Bergmeyer, H. V. (1983) *Methods Enzym. Anal.* 11, 173.
- Clark, J. D., O'Keefe, S. J., & Knowles, J. R. (1988) *Biochemistry* 27, 5961.
- Eggerer, H. (1965) *Biochem. Z.* 343, 111.
- El-Kettani, M. A. E.-C., Zakrzewska, K., Durup, J., & Lavery, R. (1993) *Proteins* 16, 393.
- Evans, C. T., Owens, D. D., Slaughter, C. A., & Srere, P. A. (1988a) *Biochem. Biophys. Res. Commun.* 157, 1231.
- Evans, C. T., Owens, D. D., Sumegi, B., Kispal, G., & Srere, P. A. (1988b) *Biochemistry* 27, 4680.
- Gerstein, M., Lesk, A. M., & Chothia, C. (1994) *Biochemistry* 33, 6739.
- Hammond, D. C., Kruggel, W. G., Lewis, R. V., & Barden, R. E. (1986) *J. Biol. Chem.* 261, 8424.
- Karpusas, M., Branchaud, B., & Remington, S. J. (1990) *Biochemistry* 29, 2213.

- Karpusas, M., Holland, D., & Remington, S. J. (1991) *Biochemistry* 30, 6024.
- Kollmann-Koch, A., & Eggerer, H. (1989) *Eur. J. Biochem.* 185, 441.
- Koshland, D. E., Jr., Nemethy, G., & Filmer, D. (1966) *Biochemistry* 5, 365.
- Kurz, L. C., & Drysdale, G. R. (1987) *Biochemistry* 26, 2623.
- Kurz, L. C., Ackerman, J. J. H., & Drysdale, G. R. (1985) *Biochemistry* 24, 452.
- Kurz, L. C., Shah, S., Crane, B. R., Donald, L. J., Duckworth, H. W., & Drysdale, G. R. (1992a) *Biochemistry* 31, 7899.
- Kurz, L. C., Drysdale, G. R., Riley, M. C., Evans, C. T., & Srere, P. A. (1992b) *Biochemistry* 31, 7908.
- Lill, U., Schreil, A., Henschen, A., & Eggerer, H. (1983) *Eur. J. Biochem.* 143, 205.
- Lill, U., Bibinger, A., & Eggerer, H. (1987a) *Eur. J. Biochem.* 162, 683.
- Lill, U., Bibinger, A., & Eggerer, H. (1987b) *Eur. J. Biochem.* 163, 599.
- Löhlein, G., & Eggerer, H. (1982) *Hoppe-Seyler's Z. Physiol. Chem.* 363, 1103.
- Löhlein-Werhahn, G., Bayer, E., Bauer, B., & Eggerer, H. (1983) *Eur. J. Biochem.* 133, 665.
- Löhlein-Werhahn, G., Goepfert, P., & Eggerer, H. (1985) *Eur. J. Biochem.* 150, 79.
- Löhlein-Werhahn, G., Goepfert, P., Kollmann-Koch, A., & Eggerer, H. (1988) *Biol. Chem. Hoppe-Seyler* 369, 417.
- Lynen, F. (1960) *Methods Enzymol.* 5, 444.
- Meyers, J. A., & Boyer, P. D. (1984) *Biochemistry* 23, 1264.
- Monod, J., Wyman, J., & Changeux, J.-P. (1965) *J. Mol. Biol.* 12, 88.
- Neet, K. E. (1980) *Methods Enzymol.* 64, 139.
- Ohashi, K., Otsuka, H., & Seyama, Y. (1985) *J. Biochem.* 97, 867.
- Pettersson, G., Lill, U., & Eggerer, H. (1989) *Eur. J. Biochem.* 182, 119.
- Remington, S., Wiegand, G., & Huber, R. (1982) *J. Mol. Biol.* 158, 111.
- Ricard, J., Meunier, J.-C., & Buc, J. (1974) *Eur. J. Biochem.* 49, 195.
- Riddles, P. W., Blakeley, R. L., & Zerner, B. (1979) *Anal. Biochem.* 94, 75.
- Srere, P. A. (1966) *J. Biol. Chem.* 241, 2157.
- Srere, P. A. (1967) *Biochem. Biophys. Res. Commun.* 26, 609.
- Srere, P. A. (1969) *Methods Enzymol.* 14, 3.
- Weidman, S. W., & Drysdale, G. R. (1979) *Biochem. J.* 177, 169.
- Wiegand, G., & Remington, S. (1986) *Ann. Rev. Biophys. Biophys. Chem.* 15, 97.
- Wiegand, G., Remington, S., Deisenhofer, J., & Huber, R. (1984) *J. Mol. Biol.* 174, 205.
- Zhi, W., Srere, P. A., & Evans, C. T. (1991) *Biochemistry* 30, 9281.
- Zimmerle, C. T., & Frieden, C. (1989) *Biochem J.* 258, 381.

BI9510082